HHS Public Access

Author manuscript

Cell Rep. Author manuscript; available in PMC 2021 November 28.

Published in final edited form as:

Cell Rep. 2021 October 05; 37(1): 109789. doi:10.1016/j.celrep.2021.109789.

Attenuation of apoptotic cell detection triggers thymic regeneration after damage

Sinéad Kinsella[1,2,*], **Cindy A. Evandy**[1,2], **Kirsten Cooper**[1,2], **Lorenzo Iovino**[1,2], **Paul C. deRoos**[1,2], **Kayla S. Hopwo**[1,2], **David W. Granadier**[1,2], **Colton W. Smith**[1,2], **Shahin Rafii**[3], **Jarrod A. Dudakov**[1,2,4,5,*]

[1]Program in Immunology, Clinical Research Division, Fred Hutchinson Cancer Research Center, Seattle, WA 98109, USA

[2]Immunotherapy Integrated Research Center, Fred Hutchinson Cancer Research Center, Seattle, WA 98109, USA

[3]Department of Genetic Medicine and Ansary Stem Cell Institute, Weill Cornell Medical College, New York, NY 10021, USA

[4]Department of Immunology, University of Washington, Seattle, WA 98109, USA

[5]Lead contact

SUMMARY

The thymus, which is the primary site of T cell development, is particularly sensitive to insult but also has a remarkable capacity for repair. However, the mechanisms orchestrating regeneration are poorly understood, and delayed repair is common after cytoreductive therapies. Here, we demonstrate a trigger of thymic regeneration, centered on detecting the loss of dying thymocytes that are abundant during steady-state T cell development. Specifically, apoptotic thymocytes suppressed production of the regenerative factors IL-23 and BMP4 via TAM receptor signaling and activation of the Rho-GTPase Rac1, the intracellular pattern recognition receptor NOD2, and micro-RNA-29c. However, after damage, when profound thymocyte depletion occurs, this TAM-Rac1-NOD2-miR29c pathway is attenuated, increasing production of IL-23 and BMP4. Notably, pharmacological inhibition of Rac1-GTPase enhanced thymic function after acute damage. These findings identify a complex trigger of tissue regeneration and offer a regenerative strategy for restoring immune competence in patients whose thymic function has been compromised.

[*]**Correspondence:** skinsell@fredhutch.org (S.K.), jdudakov@fredhutch.org (J.A.D.).

AUTHOR CONTRIBUTIONS

S.K. designed, executed, analyzed, and interpretated all of the studies as well as drafting and writing the manuscript; C.E. performed many of the *in vitro* experiments with exECs; K.C. performed bioinformatics and *in vitro* studies; L.I., P.C.d., K.S.H., D.W.G., and C.S. performed, analyzed, and helped interpret experiments; S.R. provided vectors and guidance on the generation of exECs; J.A.D. designed, interpreted, analyzed, and supervised all studies and wrote the manuscript. All authors contributed toward editing the manuscript.

DECLARATION OF INTERESTS

S.K. and J.A.D. have filed a patent application on this work.

SUPPLEMENTAL INFORMATION

Supplemental information can be found online at https://doi.org/10.1016/j.celrep.2021.109789.

Graphical Abstract

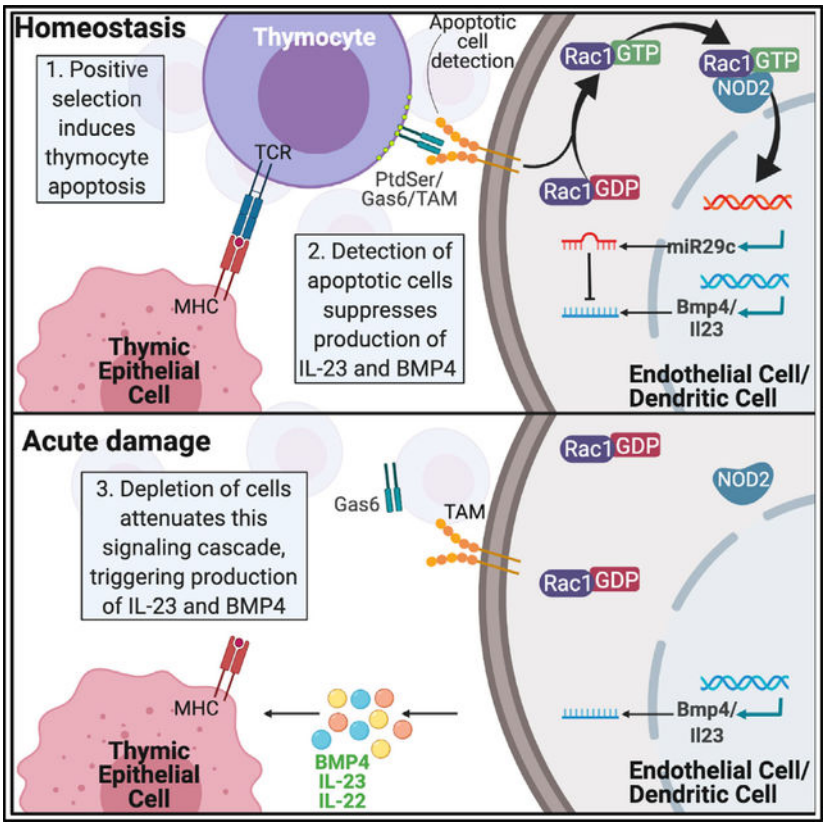

In brief

Delayed lymphopenia is a common feature of many cancer therapies that is predicated on poor regeneration of thymic function. Kinsella et al. identify a trigger of endogenous thymic repair, centered on the detection of apoptotic thymocytes, that can be exploited to improve T cell regeneration after immune-depleting therapies.

INTRODUCTION

Efficient functioning of the thymus is critical for establishing and maintaining effective adaptive immunity (Miller, 2020). T cell development is a highly complex process involving cross-talk between developing thymocytes and the non-hematopoietic supporting stromal microenvironment, primarily highly specialized thymic epithelial cells (TECs), but also endothelial cells (ECs), fibroblasts, and dendritic cells (DCs) (Abramson and Anderson, 2017). The thymus is exceptionally sensitive to negative stimuli that, together with its well-characterized capacity for repair, leads to continual cycles of involution and regeneration in response to acute injury (Gruver and Sempowski, 2008; Kinsella and Dudakov, 2020; van den Broek et al., 2016). However, this endogenous regenerative aptitude declines with age as a function of thymic involution leading to a reduced ability to respond to new pathogens, as well as poor response to vaccines and immunotherapy (Granadier et al., 2021; Velardi et al., 2020). Therefore, there is a pressing clinical need for the development of therapeutic

strategies that can enhance T cell reconstitution. One approach is to exploit key pathways that promote endogenous thymic regeneration into pharmacologic strategies; however, the molecular mechanisms governing endogenous thymic regeneration are not fully understood.

Recent studies have revealed that endogenous thymic repair is dependent on the production of two distinct regeneration factors, interleukin-23 (IL-23) and BMP4, by DCs and ECs, respectively (Dudakov et al., 2012, 2017; Wertheimer et al., 2018). Both IL-23 and BMP4 target TECs to facilitate regeneration, the former through the downstream production of IL-22 by innate lymphoid cells (ILCs) (Buonocore et al., 2010; Cella et al., 2009; Dudakov et al., 2012, 2017; Wertheimer et al., 2018; Zheng et al., 2007). These regeneration-associated factors have profound reparative effects in the thymus after acute injury and can be utilized individually as therapeutic strategies of immune regeneration (Kinsella and Dudakov, 2020). Although BMP4 and the IL-23-IL-22 axis represent two regenerative pathways that facilitate TEC repair, both the damage-sensing mechanisms that trigger the production of these factors and the molecular pathways that intrinsically regulate *Bmp4* and *Il23* expression after damage are unknown.

Here, we identify an innate trigger of the reparative response in the thymus, centered on the attenuation of signaling directly downstream of apoptotic cell detection as thymocytes are depleted after acute damage. We found that the intracellular pattern recognition receptor NOD2, via induction of microRNA-29c, suppressed levels of the regenerative factors IL-23 and BMP4, in DCs and ECs, respectively. During steady-state T cell development, a high proportion of thymocytes undergo apoptosis due to selection events during T cell development (Hernandez et al., 2010; Jameson et al., 1995). We demonstrate that this provides a signal for a suppressive pathway that is constitutively activated by the detection of exposed phosphatidylserine on apoptotic cells by cell-surface TAM receptors (Rothlin et al., 2015) on DCs and ECs, with downstream intracellular activation of the Rho GTPase Rac1. However, after damage, when profound cell depletion occurs across the thymus, the TAM-Rac1-NOD2-miR29c pathway is abrogated in the absence of apoptotic thymocytes, therefore allowing for the increased production of IL-23 and BMP4. Importantly, this pathway could be modulated pharmacologically by inhibiting Rac1 GTPase activation *in vivo*, which resulted in increased thymic function and T cell recovery after acute damage. In conclusion, this work not only represents an innovative regenerative strategy for restoring immune competence in patients whose thymic function has been compromised due to cytoreductive conditioning, infection, or age but also identifies a mechanism by which tissue regenerative responses are triggered.

RESULTS

NOD2 negatively regulates thymus regeneration by suppressing the production of BMP4 and IL-23

To identify potential mechanisms by which thymic regeneration networks are governed, we first performed transcriptome analysis on purified ECs (the primary source of BMP4 after damage [Wertheimer et al., 2018]) isolated from the mouse thymus at days 0 and 4 after a sublethal dose of total body irradiation (SL-TBI, 550 cGy), time points that capture baseline expression levels and expression at the initiation of the regenerative response

(day 4) (Dudakov et al., 2012; Wertheimer et al., 2018). Analysis through the DAVID bioinformatics tool revealed a surprising number of pathways associated with immune function, which included most of the pathways with a false discovery rate [FDR] of <0.05 (Figures 1A and S1A). Further analysis identified that, within these pathways, several genes shared a high frequency across all gene ontology (GO) pathways (Figure 1A). In particular, nucleotide-binding oligomerization domain-containing protein 2 (NOD2) stood out not only as it is centrally involved in innate immunity via its role in detection of danger signals, such as bacterial peptidoglycan (Caruso et al., 2014; Chen et al., 2009) but also because NOD2 is one of the only molecular pathways previously reported to suppress the production of IL-23 by DCs (Brain et al., 2013). Notably, GSEA analysis supported the role of NOD2 in the damage response, with a significant enrichment in the signature of downstream NOD2 gene targets (Billmann-Born et al., 2011) at day 4 after damage (Figure S1B). Importantly, transcriptome analysis in highly purified DCs after damage revealed highly similar inflammatory gene signatures and enrichment for NOD2 expression (Figures 1B and S1C). Although the expression of *Nod2* in thymic tissue has been known for some time (Iwanaga et al., 2003), the only functional role for NOD2 that has been described in the thymus has been in thymocyte selection (Martinic et al., 2017). Therefore, we hypothesized that NOD2 activation was central to the inhibition of IL-23 and BMP4, and after damage this activation is abrogated upstream by the depletion of thymocytes. To explore the effects of NOD2 deficiency on thymic regeneration following insult, wild-type (WT) or *Nod2*$^{-/-}$ animals were exposed to SL-TBI, and levels of thymic IL-23 and BMP4 were measured by ELISA. *Nod2*$^{-/-}$ thymi had increased absolute intracellular levels of BMP4 and IL-23 compared to WT controls after damage (Figure 1C). Downstream of IL-23, we also found a significant increased production of IL-22 in Nod2-deficient thymi (Figure S2A). Consistent with this, there was a commensurate increase in thymic cellularity, from as early as 7 days after SL-TBI (Figure 1D), suggesting that these increased levels of regenerative factors are supporting superior thymic regeneration. Although there was no global change in thymocyte proportions (Figure 1E), the enhanced total cellularity was reflected by increases in all subsets of thymocytes (Figure 1F). Remarkably, given their role in the production of the regenerative factors, there was no change in the number of ECs in the *Nod2*-deficient thymus; however, we observed increased regeneration of CD103^{+} DCs in *Nod2*$^{-/-}$ thymi, compared with WT (Figure 1G), which mediate IL-23 levels (Dudakov et al., 2012; Kinnebrew et al., 2012). Importantly, given the increased levels of BMP4 and IL-23, which can directly or indirectly induce TEC proliferation and function (Dudakov et al., 2012; Wertheimer et al., 2018), there was significantly augmented regeneration of both cortical TECs (cTECs) and medullary TECs (mTECs) (Figure 1H), both of which have distinct crucial roles in T cell development (Abramson and Anderson, 2017). Elevated thymic function persisted in mice deficient for NOD2 compared to age-matched WT controls even 150 days after TBI (Figure 1I); although perhaps prolonged effects are not surprising given that *Nod2*-deficient mice exhibited increased levels of IL-23 and BMP4 even at baseline (Figure S2B), which was also reflected by enhanced baseline cellularity and individual thymocyte subsets (Figures S2C–S2E).

miR29c mediates the suppressive function of NOD2

NOD2 has been previously shown to induce expression of the microRNA miR29, which downregulates IL-23 by directly regulating transcription of *Il12p40* and indirectly regulating *Il23p1*9 (Brain et al., 2013). MicroRNAs are small non-coding RNAs that critically govern protein expression by binding to and degrading target RNA (Bartel, 2004; Krol et al., 2010; Makeyev and Maniatis, 2008). There are three members of the miR29 family, each with some overlapping physiological functions, including a TEC-intrinsic role of *miR29*a in regulating the response to interferon signaling and Aire-dependent gene expression (Papadopoulou et al., 2011; Ucar et al., 2013). Furthermore, the expression of all three miR29 family members are increased in the aged thymus, suggesting a potential role in involution (Ye et al., 2014). To understand whether miR29 was involved in the regenerative response in the thymus, we first assessed the expression levels of mature 3p and 5p arms of *miR29a*, *miR29b*, and *miR29c* in the thymus from WT or *Nod2*$^{-/-}$ mice 3 days after TBI and found lower expression of *miR29c-5p* in *Nod2*-deficient mice (Figure 2A). To elucidate whether there was a cell-specific function of miR29 in the thymus, we assessed miR29 expression in purified populations of ECs, DCs, and DP thymocytes and did not find a significant change in the expression of either *miR29a-5p* or *miR29b-5p* after damage (Figure S3A). However, we observed decreased expression of *miR29c-5p* in ECs and DCs after damage, with this damage-induced reduction lacking in DP thymocytes (Figure 2B), suggesting an endogenous regulation in *miR29c-5p* after damage in the regeneration-initiating DCs and ECs, both of which have higher *miR29c-5p* expression at baseline compared to DP thymocytes (Figure S3B).

To functionally assess the relationship between miR29c-5p and the production of regenerative factors, we used a technique to constitutively activate the Akt pathway in freshly isolated thymic ECs using the pro-survival adenoviral gene *E4ORF1*, which allows for their *ex vivo* propagation and expansion while maintaining endothelial phenotype, adaptability, as well as vascular tube formation capacity (Seandel et al., 2008; Wertheimer et al., 2018), allowing for functional manipulation of the cells for *in vitro* modeling of regenerative pathways. Consistent with the decrease of *miR29c-5p* in regeneration-initiating cells after damage, and the previously identified role of miR29 in the attenuation of *Il23p19* (Brain et al., 2013), we hypothesized that miR29c-5p regulates the expression of *Bmp4* in ECs. Overexpression of *miR29c-5p* in thymic exECs resulted in a significant reduction in the expression of *Bmp4* (Figure 2C). Conversely, Bmp4 expression was increased upon inhibition of *miR29c-5p* (Figure 2D). Importantly, freshly isolated DCs transfected with a *miR29c-5p* mimic demonstrated a similar reduction in expression of the *Il23p19* subunit (Figure 2E), suggesting that *miR29c-5p* negatively regulates these regenerative factors in both ECs and DCs. miRNAs regulate gene expression in several ways, either by binding to the 3′ UTR of their target transcript and inducing post-transcriptional modifications and translational repression, ultimately resulting in transcript degradation, or by binding to the 5′ UTR sequence of their target transcript and exerting silencing effects on gene expression (Huntzinger and Izaurralde, 2011). To understand whether *miR29c-5p* regulation of *Bmp4* and *Il23p19* was due to direct binding, and to determine where this binding occurred, we carried out a luciferase assay using 3′UTR and 5′ UTR *Bmp4*-luciferase constructs that were co-transfected with a *miR29c-5p* mimic. We observed a degradation of the 3′

UTR of *Bmp4* in the presence of the *miR29c-5p* mimic, identifying a direct and specific regulation of *miR29c-5p* on *Bmp4* expression (Figure 2F), with a suggested indirect effect of *miR29c-5p* on *Il23p19* stability, consistent with previous reports (Papadopoulou et al., 2011).

Detection of apoptotic thymocytes by TAM receptors suppresses the production of regenerative factors

Although we have demonstrated that attenuation of NOD2-dependent *miR*29c-5p expression is involved in regulating levels of critical regenerative factors, the upstream initiator of this cascade is not defined. In our previous studies, we found a link between the loss of thymic cellularity and the initiation of the IL-22 and BMP4 pathways (Dudakov et al., 2012, 2017; Wertheimer et al., 2018). In the case of IL-22/IL-23, this could be directly correlated with the depletion in the number of $CD4^+CD8^+$ double-positive (DP) thymocytes, as mice with a genetic block before the DP stage (*Rag1*$^{-/-}$, *Il7ra*$^{-/-}$, *Il7*$^{-/-}$, and *Tcrb*$^{-/-}$) (Mak et al., 2001) or mice treated with dexamethasone, which causes a targeted reduction in DP thymocytes (Purton et al., 2004), expressed profoundly more IL-22 and IL-23 than WT controls or mutant mice with blocks further downstream in T cell development (*Tcra*$^{-/-}$ and *Ccr7*$^{-/-}$) (Dudakov et al., 2012). In the case of the mutant mouse strains, this occurred even without acute thymic damage, suggesting that merely the absence of DP thymocytes is enough to trigger these reparative pathways. Although 80%–90% of the thymus comprises DP thymocytes, approximately 99% of these cells undergo apoptosis under homeostatic conditions due to selection events (Hernandez et al., 2010; Jameson et al., 1995). Taken together with reports that apoptotic cells can regulate the production of cytokines, including reducing the production of IL-23 by DCs (Municio et al., 2011), we hypothesized that the presence of homeostatic apoptotic thymocytes can limit the production of the regenerative factors IL-23 and BMP4. To test this, we performed co-culture experiments of thymocytes with thymic ECs or DCs, where the thymocytes had been further induced to undergo apoptosis with dexamethasone (Cifone et al., 1999) (referred to as apoptotic cells, ACs), or where apoptosis was inhibited with the pan-caspase inhibitor z-VAD-FMK, which considerably reduced thymocyte apoptosis as measured by Annexin V binding (Figure S4A). Consistent with the hypothesis that ACs suppress the production of regenerative factors, inhibiting apoptosis in thymocytes significantly enhanced the production of *Bmp4* in ECs and IL-23 in DCs (Figures 3A and 3B). Annexin V is a surrogate marker of apoptotic cells and binds to exposed phosphatidylserine (PtdSer), inversion of which from the inner cell membrane is a key identifying feature of apoptotic cells (Mower et al., 1994; Schlegel et al., 1993). Even though on a per-cell basis there is an increase in Annexin V binding on DP thymocytes after damage (Figure 3C), given the severe depletion in DP thymocytes after damage (Figures 3D and 3E) there was a profound decrease in total exposed PtdSer (Figures 3F, S4B, and S4C), resulting in a robust correlation between exposed PtdSer and DP cellularity (Figure 3G). Apoptotic cell clearance can be facilitated by the detection of exposed PtdSer by the TAM receptors, Tyro, Axl, and Mer, on nearby cells. TAM receptors are a family of transmembrane tyrosine kinase receptors that recognize their extracellular ligands Gas6 or ProS 1 in the presence of PtdSer and have a critical role in the maintenance of immune homeostasis, including regulation of thymic negative selection (Lemke and Rothlin, 2008; Rothlin et al., 2015; Wallet et al., 2009). Both thymic ECs and DCs express

Axl, Mer, and *Tyro3* (Figure 3H), as has been extensively reported previously in other tissues (Rothlin et al., 2015). Consistent with the inhibition of apoptosis, abrogation of TAM receptor signaling with the pan-inhibitor RXDX-106 (Yokoyama et al., 2019) increased expression of *Bmp*4 in ECs and IL-23 in DCs (Figures 3I and 3J).

TAM receptor signaling promotes Rac1 GTPase activation and limits *Bmp4* and *Il23*

PtdSer guides and strengthens ligand binding to TAM receptors and is critical for TAM receptor activation and downstream signaling (Rothlin et al., 2015). One of the common downstream targets of TAM receptors are Rho GTPases, which is notable given recent reports that, in addition to its capacity to sense bacterial-derived peptidoglycans, NOD2 can also act as a cytosolic sensor of activated Rho GTPases (Keestra et al., 2013; Keestra-Gounder and Tsolis, 2017). Rho GTPases have multiple cellular roles centered on modulation of the cellular cytoskeletal architecture and regulate processes such as cell adhesion, migration, polarization, and trafficking (Hervé and Bourmeyster, 2015). To investigate the role of Rho GTPases in the regulation of regenerative factors, we first performed a functional screen of inhibitors of Rho, Rac, and Cdc42 subclasses of Rho GTPases (Hervé and Bourmeyster, 2015; Hodge and Ridley, 2016; Lin and Zheng, 2015) in exECs or freshly isolated thymic DCs and assessed the expression of regenerative factors. Using this approach, we identified that, while inhibition of Cdc42 did not mediate considerable effects on the production of *Bmp4* by ECs or *Il12p40* in DCs, inhibition of Rac1 led to significantly increased expression in these regenerative factors (Figures 4A and 4B). Interestingly, inhibition of ROCK1, a downstream mediator of RhoA, induced *Bmp4* but not *Il12p40*, although RhoA itself only trended toward an increase in Bmp4 production. Given the common profound effect of Rac1 inhibition across ECs and DCs in these *in vitro* assays, we next sought to determine whether detection of apoptotic thymocytes could indeed lead to Rac1 GTPase activation. Consistent with our proposed framework, we demonstrated that inhibiting either the induction of apoptosis or the detection of apoptotic thymocytes reduced activation of Rac1 in thymic ECs (Figures 4C and 4D). Notably, we found significantly increased thymic recovery following acute injury caused by SL-TBI in Rac1 was deleted in mice specifically from DCs (Figure 4E).

Rac1 GTPase inhibition enhances thymus regeneration and thymic output *in vivo*

Several strategies targeting Rho GTPases have been examined pre-clinically for multiple cancers. These include small molecules targeting the spatial regulation of GTPase activators (Mazieres et al., 2004), and Rho-GEF interactions, such as Rhosin (Shang et al., 2012), and our therapeutic candidate Rac1 GTPase inhibitor EHT1864 (Shutes et al., 2007), with the greatest clinical trial success thus far in targeting the downstream kinase of RhoA, ROCK (Dong et al., 2010; Sadok et al., 2015). To determine whether this pathway could be manipulated for therapeutic efficacy in thymic regeneration, we treated mice with the Rac1 GTPase inhibitor EHT1864 following SL-TBI and identified a robust regeneration of thymic cellularity (Figure 5A). EHT1864 had no effect on thymus cellularity in *Nod2*$^{-/-}$ mice (Figure 5A), supporting our hypothesis of a Rac1-NOD2 regeneration axis. Although thymocyte proportions were unaffected by treatment with EHT1864 (Figure 5B), we found a similar increase in almost all thymocyte subsets (Figure 5C), which was not observed in EHT1864-treated *Nod2*-deficient mice (Figure S5). Consistent with our proposed

mechanism, we found a significant decrease in *miR29c*-5p expression in the thymus after Rac1 inhibition (Figure 5D), with a corresponding increase in the levels of BMP4 and IL-23 (Figure 5E). This was also then accompanied by enhanced TEC regeneration after EHT1864 treatment (Figure 5F). In the periphery, while there was no change in the total number of $CD4^+$ or $CD8^+$ thymocytes or their relative proportions (Figures 5G and 5H), there was an increase in the output of naive T cells in mice treated with EHT1864, reflected by their proportion and the ratio of naive:memory cells (Figures 5I and 5J).

DISCUSSION

Despite its importance for generating a competent repertoire of T cells, the thymus is exquisitely sensitive to acute injury such as that caused by infection, shock, or common cancer therapies such as cytoreductive chemo- or radiation therapy; however, it also has a remarkable capacity for repair (Dudakov et al., 2012; Gruver and Sempowski, 2008). Even in the clinical setting where children who have had large parts of their thymus removed exhibit significant thymic repair (van den Broek et al., 2016). Of note, the general phenomena of endogenous thymic regeneration has been known for longer even than its immunological function (Jaffe, 1924; Miller, 1961); however, the underlying mechanisms controlling this process are poorly understood (Chidgey et al., 2007; Dudakov et al., 2010). Thus, endogenous thymic regeneration is a critical process to restore immune competence following thymic injury, although acute and profound thymic damage such as that caused by common cancer cytoreductive therapies, conditioning regimes as part of hematopoietic cell transplantation (HCT), or age-related thymic involution lead to prolonged T cell deficiency, precipitating high morbidity and mortality from opportunistic infections and may even facilitate cancer relapse (Bosch et al., 2012; Clave et al., 2013; Dudakov et al., 2016; Komanduri et al., 2007; Legrand et al., 2007; Mackall, 2000; Mackall et al., 1995; Parkman and Weinberg, 1997; Pizzo et al., 1991; van den Brink et al., 2018; Weinberg et al., 1995; Williams et al., 2007). Recent studies have shown that thymic ILCs and ECs have profound reparative effects in the thymus after acute injury through their production of the regeneration-associated factors IL-22 and BMP4, respectively, both of which act by stimulating TECs (Dudakov et al., 2012, 2017; Wertheimer et al., 2018). Although activation of these reparative programs was linked with the depletion of thymocytes, hinting at an innate trigger of regeneration, the mechanisms that controlled this response were unclear. In this study, we reveal that apoptotic thymocytes, which are abundant as a result of selection events during tolerance induction (Hernandez et al., 2010; Jameson et al., 1995), signaling through TAM receptors and the downstream activation of Rac1 GTPase, NOD2, and miR29c, actively suppresses the steady-state production BMP4 and IL-23, the upstream regulator of IL-22 production.

One of the ways that apoptotic cells are detected is via the receptor tyrosine kinases Tyro3, Axl, and Mertk (TAM). TAM receptors are pivotal mediators of innate immunity, detecting exposed PtdSer on apoptotic cells via the intermediaries Gas6 or Pros1 (Lemke and Rothlin, 2008; Rothlin et al., 2015). In addition to being crucial for promoting phagocytosis of apoptotic cells, TAM receptor signaling has been also shown to limit the innate immune response, particularly in the suppression of cytokine production (Chan et al., 2016; Rothlin et al., 2007). However, TAM receptors can also act as a rheostat for controlling the activity

of pleiotropic cytokines such as IL-4 and IL-13 (Bosurgi et al., 2017). This framework for TAM receptor regulation of immune responses is consistent with our findings that PtdSer detection by TAM receptors on thymic ECs and DCs inhibits their expression of BMP4 and IL-23, respectively. However, after damage, the loss of thymocytes (and their exposed PtdSer) attenuates this tonic signaling, inducing the production of regenerative factors. Moreover, given the passive activation of this pathway, this acts as a "dead-man's switch" that ensures faithful regulation and activation of the regeneration program in settings of damage.

Notably, while expression of *Nod2* in the thymus has been known for some time (Iwanaga et al., 2003), it has thus far only been functionally linked to positive selection and maturation of $CD8^+$ T cells by facilitating TCR-ERK signaling (Martinic et al., 2017). Reports suggest that NOD2 can control the production of IL-23 by DCs via miR29, which directly regulated the transcription of *Il12p40* and indirectly through *Il23p1*9 (Brain et al., 2013). The three members of the miR29 family have overlapping physiological roles, and a role for TEC-intrinsic miR29a/b has been described in tuning the epithelial response to injury by controlling IFN receptor expression (Papadopoulou et al., 2011). However, here, we revealed that EC and DC-intrinsic miR29c facilitates NOD2-mediated suppression of thymic regeneration directly by suppressing *Bmp4* expression, and indirectly regulating both p19 and p40 subunits of IL-23. Although we can detect all three miR29 family members in DP thymocytes, ECs, and DCs, expression of miR29c-5p was significantly higher in ECs and DCs, and there was a targeted decrease in expression within ECs and DCs after TBI but not DPs thymocytes.

The canonical ligands for NOD2 are peptidoglycans found in the cell wall of bacteria (Caruso et al., 2014); however, these are unlikely to serve as a NOD2 activator in the thymus since it is typically thought of as a sterile organ (Nunes-Alves et al., 2013). One recently described alternate function of NOD2 is as a cytosolic sensor of activated Rho GTPases (Keestra et al., 2013; Keestra-Gounder and Tsolis, 2017; Legrand-Poels et al., 2007). This is especially notable given the role that Rho-GTPase activation plays in TAM receptor signaling (Mao and Finnemann, 2015; Todt et al., 2004; Wu et al., 2005). The Rho GTPase family is responsible for a wide range of physiological processes (Hodge and Ridley, 2016; Van Aelst and D'Souza-Schorey, 1997; Wennerberg and Der, 2004), including the intrathymic regulation by Rac1, RhoA, and Cdc42 of β-selection and positive selection (Gomez et al., 2001; Gomez et al., 2000). Rho GTPases including RhoA, Rac1, and Cdc42 can be activated by caspase-3 during apoptosis (Coleman and Olson, 2002; Krieser and Eastman, 1999; Na et al., 1996) and themselves further promote apoptosis (Koyanagi et al., 2008; Lacal, 1997; Sanno et al., 2010), including in thymocytes that do not successfully express a pre-TCR (Dumont et al., 2009). Notably, both NOD2-miR29 and apoptotic cells have been identified to negatively regulate the production of IL-23 by DCs (Brain et al., 2013; Municio et al., 2011).

Prolonged thymic repair following everyday insults represents an important clinical problem in older patients. Several strategies targeting Rho GTPases have been examined pre-clinically for multiple cancers. These include small molecules targeting the spatial regulation of GTPase activators (Mazieres et al., 2004), and Rho-GEF interactions, such as Rhosin

(Shang et al., 2012) and EHT1864 (Shutes et al., 2007). Furthermore, there is considerable interest in the effect of ROCK inhibition on T cell function, particularly during graft versus host disease and autoimmunity (Flynn et al., 2016; Jagasia et al., 2021; Ricker et al., 2016; Zanin-Zhorov et al., 2014). We have found that these Rho-GTPase pathways can be effectively targeted therapeutically to boost thymic function and peripheral T cell reconstitution. Several Rho GTPases, including Rac1, RhoA, and Cdc42, play a role in T cell development (Gomez et al., 2001; Gomez et al., 2000), notably during stages of selection when there are high levels of apoptosis (Hernandez et al., 2010), implying a potential down-side to Rho GTPase inhibition. However, given the proposed therapeutic window coincides with when thymocytes are largely absent, together with the redundancy of Rac1 and Rac2 in T cell development (Guo et al., 2008), Rac1 inhibition represents a promising therapeutic strategy for boosting immune function. Interestingly, although deletion of Rac1 in TECs promotes thymic atrophy (Hunziker et al., 2011), given that Rac1 deletion also enhances myc expression that has been shown to expand TEC numbers (Cowan et al., 2019), the functional consequences of Rac1 inhibition in TECs will need to be carefully evaluated. In summary, these findings not only uncover mechanisms governing endogenous thymic repair; considering the previously highlighted roles of BMP signaling as well as the IL-23/IL-22 axis in the repair of several tissues, such as intestine, liver, bone, muscle, and skin (Dudakov et al., 2015; Parikh et al., 2011; Schmidt-Bleek et al., 2016), these findings outline a potentially globally applicable pathway triggering tissue regeneration. Furthermore, by targeting this pathway pharmacologically, we propose a therapeutic intervention that could be used to boost immune function in patients whose thymus has been damaged due to age, cytoreductive therapies, infection, or other causes.

STAR★METHODS

Detailed methods are provided in the online version of this paper and include the following:

RESOURCE AVAILABILITY

Lead contact—Further information and requests for resources and reagents should be directed to and will be filled by the Lead Contact, Jarrod Dudakov (jdudakov@fredhutch.org).

Materials availability—This study did not generate new unique reagents.

Data and code availability—The microarray and RNA sequencing datasets described in this manuscript have been deposited in GEO and are available as of the date of publication at GEO: GSE106982, GSE160989, and GSE183056.

This manuscript does not report original code.

Any additional information required to reanalyze the data reported in this paper is available from the lead contact upon request.

EXPERIMENTAL MODEL AND SUBJECT DETAILS

Mice—Inbred male and female C57BL/6J mice were obtained from the Jackson Laboratories (Bar Harbor, USA). *Nod2*$^{-/-}$ (B6.129S1-*Nod2*^{tm1Flv}/J) mice were obtained from Jackson Laboratories and bred in house. Rac1 flox mice (Rac1^{tm1Djk}/J) and CD11c-Cre-GFP line (C57BL/6J-Tg(Itgax-cre,-EGFP)4097Ach/J) were obtained from Jackson Laboratories and crossed in house to generate Rac1$^{fl/fl}$*CD11c-Cre. All experimental mice were between 6–8 weeks old. To induce thymic damage, mice were given sub-lethal total body irradiation (SL-TBI) at a dose of 550 cGy from a cesium source mouse irradiator (Mark I series 30JL Shepherd irradiator) with no hematopoietic rescue. For *in vivo* studies of EHT-1864 administration, mice were given SL-TBI (550cGy) and subsequently received i.p. injections of 40 mg/kg EHT1864 (3872, Tocris, UK), or 1 × PBS as control, on days 3, 5 and 7 following TBI. Mice were maintained at the Fred Hutchinson Cancer Research Center (Seattle, WA), and acclimatized for at least 2 days before experimentation, which was performed per Institutional Animal Care and Use Committee guidelines.

Cell isolation—Single cell suspensions of freshly dissected thymuses were obtained and either mechanically suspended or enzymatically digested using 0.15% Collagenase D (Sigma, 11088882001) and 0.1% DNase 1 (Sigma, 10104159001) in DMEM, as previously described (Dudakov et al., 2012; Velardi et al., 2014), and counted using the Z2 Coulter Particle and Size Analyzer (Beckman Coulter, USA). For studies sorting rare populations of cells in the thymus, multiple identically-treated thymuses were pooled so that sufficient number of cells could be isolated; however, in this instance separate pools of cells were established to maintain individual samples as biological replicates.

Generation of exECs—exECs were generated as previously described (Seandel et al., 2008). Briefly, CD45^{-}CD31^{+} cells were FACS purified and incubated with lentivirus containing either the E4ORF1 or myrAkt construct for 48 hours. Cell culture medium containing 20% FBS (SH30066.03, HyClone, GE Life Sciences), 10 mM HEPES (15630–080, Invitrogen), 1% Glutamax (35050061, Life Technologies), 1% Non-Essential Amino Acids (11140050, Life Technologies), 1% PenStrep (15240–062, Invitrogen), 50 ug/ml Heparin (H3149, Sigma), 50 ug/ml Endothelial Cell Supplement (02–102, Millipore-Sigma), 5 μM SB431542 (1614/10, R&D Systems), 20 ng/ml FGF (100–18B, Peprotech) and 10 ng/ml VEGF (450–32, Peprotech) at 37°C, 5% O_2, 5% CO_2 in a HERAcell 150i incubator (Thermo Fisher, USA).

METHOD DETAILS

Reagents—Cells were stained with the following antibodies for analysis CD3-FITC (35–0031, Tonbo Bioscience), CD8-BV711 (100748, BioLegend), CD4-BV650 (100546, BioLegend), CD45-BUV395 (565967, BD Biosciences), CD90-BV785 (105331, BioLegend), CD11c-APC (20–0114, Tonbo Biosciences), MHC-II-Pac Blue (107620, BioLegend), CD103-PercPCy5.5 (121416, BioLegend), CD11b-A700 (557960, BD PharMingen), EpCAM-PercPe710 (46–5791-82, eBioscience), Ly51-PE (12–5891-83, eBioscience), CD31-PECy7 (25–0311-82, eBioscience), CD140a-APC (135907, BioLegend), UEA1-FITC (FL-1061, Vector Laboratories), TCRbeta-PECy7 (109222, BioLegend), CD62L-APC-Cy7 (104427, BioLegend), CD44-Alexa Fluor RTM700 (56–

0441-82, BioLegend), CD25-PercP-Cy5.5 (102030, BioLegend). Annexin V staining (640906, BioLegend) was performed in Annexin V binding buffer (422201, BioLegend). Flow cytometric analysis was performed on an LSRFortessa X50 (BD Biosciences) and cells were sorted on an Aria II (BD Biosciences) using FACSDiva (BD Biosciences) or FlowJo (Treestar Software).

***In vitro* cell culture—**Co-culture experiments were carried out using exECs or DCs and thymocytes harvested from mechanically dissociated thymus from untreated mice, or in the case of DC analysis whole thymus cultures were used. Harvested thymocytes were incubated with either 100 nM dexamethasone (D2915, Sigma Aldrich, Germany), or 20 μM z-VAD-FMK (2163, Tocris, UK) for 4 hours at 37°C prior to co-culture, washed twice with PBS, and resuspended in exEC media for co-culture (1×10^6 cells / well). Cells were harvested 20 hours post co-culture and prepared for either qPCR analysis or flow cytometry analysis. Thymic DCs were isolated from untreated mice using CD11c UltraPure microbeads (130–108-338, Miltenyi Biotech, USA), on enzymatically digested thymuses. DCs were cultured in DMEM (11965, GIBCO), 10% FBS (SH30066.03, HyClone, GE Life Sciences), and 1% PenStrep (15240–062, Invitrogen). For TAM receptor inhibitor studies, exECs were treated with 25 μM RXDX-106 (CEP-40783, s8570, Selleck Chemicals) 30 minutes prior to incubation with dexamethasone treated or z-VAD-FMK treated thymocytes, and *Bmp4* expression was determined by qPCR analysis 20 h post co-culture. HEK293 cells (ATCC, Manassas, VA) were cultured in DMEM (11965, GIBCO), 10% FBS (SH30066.03, HyClone, GE Life Sciences), 1% Glutamax (35050061, Life Technologies), and 1% PenStrep (15240–062, Invitrogen).

ELISA—Thymuses were homogenized in RIPA buffer (25 mM Tris pH 7.6, 150 mM NaCl, 1% NP-40, 0.1% SDS, 0.05% sodium deoxycholate, 0.5 mM EDTA) with protease inhibitors (Thermo, A32955), using a Homogenizer 150 (Fisher Scientific) at a concentration of 10 mg/ml, where protein concentration was further normalized using BCA assay. BMP4 (DY485–05, R&D Systems) and IL-23 (433704, BioLegend) levels were assessed by ELISA, and absorbance was measured on the Tecan Spark 10M (Tecan, Switzerland).

Transcriptome analysis—Microarray analysis was performed on an Affymetrix MOE 430 A 2.0 platform in triplicate for untreated as well as day 4 ECs after TBI. RNaseq was performed on freshly isolated and FACS purified DCs. To obtain sufficient RNA for every time point, thymi of several mice were pooled. All samples underwent a quality control on a bioanalyzer to exclude degradation of RNA. GSEA analysis was performed using the GSEA tool v4.1 of the Broad Institute (https://www.gsea-msigdb.org/gsea). Comparisons were made to known signaling pathways from the Gene Expression Omnibus (GEO) database (GSE226611). Pathway analysis was performed by submitting genes changed > 1.5 ($p < 0.05$) to DAVID Bioinformatics Resource v6.8(Huang da et al., 2009a, b). Transcriptome data generated from ECs and DCs at day 4 after TBI will be deposited in the GEO. EC data was generated concurrently to untreated day 0 EC data, which has already been deposited to the GEO under number GSE106982 (Wertheimer et al., 2018). The full EC dataset is

available under accession numbers GSE106982 and GSE160989, while the DC sequencing data is available under accession number GSE183056.

qPCR—RNA was extracted from exECs or DCs using a RNeasy Mini kit (74104, QIAGEN), and from sorted cells using a RNeasy Plus Micro kit (74034, QIAGEN). cDNA was synthesized using the iScript gDNA Clear cDNA Synthesis kit (1725035, Bio-Rad, USA) and a Bio-Rad C1000 Touch ThermoCycler (Bio-Rad). RNA expression was assessed in the Bio-Rad CFX96 Real Time System (Bio-Rad), using iTaq Universal SYBR Green Supermix (1725122, Bio-Rad), and the following primers: *B-Actin* (*F 5′-CACTGTCGAGTCGCGTCC-3′; R 5′-TCATCCATGGCGAACTGGTG-3′*); *Il12p40* (*F 5′-AAGGAACAGTGGGTGTCCAG-3′, R 5′-CATCTTCTTCAGGCGTGTCA-3′*); *Il23p19* (*F 5′-GACTCAGCCAACTCCTCCAG-3′*; *R 5′-GGCACTAAGGGCTCAGTCAG-3′*); *Bmp4* (*qMmuCED0046239, Bio-Rad*). miRNA was extracted from cells using an miRNeasy Mini kit (217004, QIAGEN) or miRNeasy Micro kit (1071023, QIAGEN), and cDNA was synthesized using a Taqman Advanced miRNA cDNA Synthesis kit (A28007, Thermo Fisher). miRNA expression was measured on a Bio-Rad CFX96 Real Time System (Bio-Rad), using Taqman Advanced Master Mix (4444557, Thermo Fisher) and the following primers (Thermo Fisher): miR29a-3p (mmu478587_mir); miR29b-3p (mmu481300_mir); miR29c-3p (mmu479229_mir), miR29a-5p (mmu481032_mir), miR29b-5p (mmu481675_mir), miR29c-5p (mmu481034_mir).

miRNA mimic and inhibition—miRNA overexpression or inhibition was carried out by transfection of 50 μM miRVANA miRNA mimic (4464066, Thermo Fisher) or 100 μM miRCURY LNA-inhibitor (YI04105459, Exiqon) for miR29c-5p or miR29c-3p. Transfections were carried out using Lipofectamine 2000 (11668030, Thermo Fisher) in Opti-MEM™ reduced serum media (31985070, GIBCO) for DCs, and using Nucleofector electroporation kit (VPI-1001, Lonza) for exECs (Program M-003, Nucleofector 2b, Lonza).

Luciferase assays—HEK293 cells (ATCC, Manassas, VA) were co-transfected with 100 mM miR29c-5p miRVANA miRNA mimic (4464066, ThermoFisher) using Lipofectamine and one of the following Luciferase vectors, using RNAifectin (G073, Abm); Blank-Luc [pLenti-Ubc-UTR-Dual-Luc-Blank vector (C047, Abm)]; BMP4–3′UTR [pLenti-Ubc-3′UTR-Dual-Luciferase (MT-m02780-Custom)]; IL12B-5′UTR [pLenti-Ubc-IL12B-5′UTR-Dual-luciferase]; IL23A-3′UTR [pLenti-Ubc-Dual-Luciferase (MT-M10060-Custom)]. Luciferase activity was measured after 24 hours using the Dual-Glo® Luciferase Assay System (E2920, Promega) on a Veritas microplate Luminometer (Turner BioSystems, USA).

Rho GTPase activation assays—Activated Rac1 was measured using the absorbance-based G-LISA Rac1 Activation Assay Biochem Kit (BK128, Cytoskeleton, USA). Briefly, exECs were co-cultured with thymocytes harvested from untreated mice, as described above. 24 hours after co-culture the exECs were harvested rapidly on ice, aliquoted and snap frozen using liquid nitrogen. Lysate volumes were subsequently adjusted for equal protein levels following BCA assay (23227, Pierce BCA protein assay kit, Thermo Fisher, USA), and

GTP-bound Rac1 levels were assessed according to the manufacturers protocol. Plates were read at 490 nm on a Spark 10M plate reader (Tecan, Switzerland).

QUANTIFICATION AND STATISTICAL ANALYSIS

Statistical analysis between two groups was performed with unpaired two-tailed t test. Statistical comparison between 3 or more groups in Figures 3F, 3H, 3K, and 4A was performed using a one-way ANOVA with Dunnett's or Tukey's multiple comparison test. Studies described in Figures 2C–2F, 3A, 3B, 3I, 3J, and 3L used paired analyses. All statistics were calculated using Graphpad Prism and display graphs were generated in Graphpad Prism or R. Information on replicates, error bars and statistical significance can be found in the figures and their corresponding legends.

Supplementary Material

Refer to Web version on PubMed Central for supplementary material.

ACKNOWLEDGMENTS

We gratefully acknowledge the assistance of the Flow Cytometry and Comparative Medicine Core Facilities and the support of the Immunotherapy Integrated Research Center at the Fred Hutchinson Cancer Research Center. We thank Dr. Brandon Hadland at the Fred Hutchinson Cancer Research Institute for generously providing the pCCL-PGK-myrAkt vector and Dr. Marcel van den Brink (Memorial Sloan Kettering Cancer Center) for mentorship and discussions. Graphical abstract was generated with BioRender.com. This research was supported by National Institutes of Health award numbers R00-CA176376 (J.A.D.) and R01-HL145276 (J.A.D.), Project 2 of P01-AG052359 (J.A.D.), and the NCI Cancer Center Support Grant P30-CA015704. Support was also received from a Scholar Award from the American Society of Hematology (J.A.D.), the Mechtild Harf (John Hansen) Award from the DKMS Foundation for Giving Life (J.A.D.), the Cuyamaca Foundation (J.A.D.), and the Bezos Family Foundation (J.A.D.). S.K. was supported by a New Investigator Award from the American Society for Transplantation and Cellular Therapy and Pilot Funding from the Cooperative Center for Excellence in Hematology (Fred Hutchinson Cancer Research Center) award number U54 DK106829.

REFERENCES

Abramson J, and Anderson G (2017). Thymic Epithelial Cells. Annu. Rev. Immunol 35, 85–118. [PubMed: 28226225]

Bartel DP (2004). MicroRNAs: genomics, biogenesis, mechanism, and function. Cell 116, 281–297. [PubMed: 14744438]

Billmann-Born S, Till A, Arlt A, Lipinski S, Sina C, Latiano A, Annese V, Häsler R, Kerick M, Manke T, et al. (2011). Genome-wide expression profiling identifies an impairment of negative feedback signals in the Crohn's disease-associated NOD2 variant L1007fsinsC. J. Immunol 186, 4027–4038. [PubMed: 21335489]

Bosch M, Khan FM, and Storek J (2012). Immune reconstitution after hematopoietic cell transplantation. Curr. Opin. Hematol 19, 324–335. [PubMed: 22517587]

Bosurgi L, Cao YG, Cabeza-Cabrerizo M, Tucci A, Hughes LD, Kong Y, Weinstein JS, Licona-Limon P, Schmid ET, Pelorosso F, et al. (2017). Macrophage function in tissue repair and remodeling requires IL-4 or IL-13 with apoptotic cells. Science 356, 1072–1076. [PubMed: 28495875]

Brain O, Owens BMJ, Pichulik T, Allan P, Khatamzas E, Leslie A, Steevels T, Sharma S, Mayer A, Catuneanu AM, et al. (2013). The intracellular sensor NOD2 induces microRNA-29 expression in human dendritic cells to limit IL-23 release. Immunity 39, 521–536. [PubMed: 24054330]

Buonocore S, Ahern PP, Uhlig HH, Ivanov II, Littman DR, Maloy KJ, and Powrie F (2010). Innate lymphoid cells drive interleukin-23-dependent innate intestinal pathology. Nature 464, 1371–1375. [PubMed: 20393462]

Caruso R, Warner N, Inohara N, and Núñez G (2014). NOD1 and NOD2: signaling, host defense, and inflammatory disease. Immunity 41, 898–908. [PubMed: 25526305]

Cella M, Fuchs A, Vermi W, Facchetti F, Otero K, Lennerz JK, Doherty JM, Mills JC, and Colonna M (2009). A human natural killer cell subset provides an innate source of IL-22 for mucosal immunity. Nature 457, 722–725. [PubMed: 18978771]

Chan PY, Carrera Silva EA, De Kouchkovsky D, Joannas LD, Hao L, Hu D, Huntsman S, Eng C, Licona-Limón P, Weinstein JS, et al. (2016). The TAM family receptor tyrosine kinase TYRO3 is a negative regulator of type 2 immunity. Science 352, 99–103. [PubMed: 27034374]

Chen G, Shaw MH, Kim YG, and Nuñez G (2009). NOD-like receptors: role in innate immunity and inflammatory disease. Annu. Rev. Pathol 4, 365–398. [PubMed: 18928408]

Chidgey A, Dudakov J, Seach N, and Boyd R (2007). Impact of niche aging on thymic regeneration and immune reconstitution. Semin. Immunol 19, 331–340. [PubMed: 18024073]

Cifone MG, Migliorati G, Parroni R, Marchetti C, Millimaggi D, Santoni A, and Riccardi C (1999). Dexamethasone-induced thymocyte apoptosis: apoptotic signal involves the sequential activation of phosphoinositide-specific phospholipase C, acidic sphingomyelinase, and caspases. Blood 93, 2282–2296. [PubMed: 10090938]

Clave E, Lisini D, Douay C, Giorgiani G, Busson M, Zecca M, Moretta F, Acquafredda G, Brescia LP, Locatelli F, and Toubert A (2013). Thymic function recovery after unrelated donor cord blood or T-cell depleted HLA-haploidentical stem cell transplantation correlates with leukemia relapse. Front. Immunol 4, 54. [PubMed: 23459761]

Coleman ML, and Olson MF (2002). Rho GTPase signalling pathways in the morphological changes associated with apoptosis. Cell Death Differ. 9, 493–504. [PubMed: 11973608]

Cowan JE, Malin J, Zhao Y, Seedhom MO, Harly C, Ohigashi I, Kelly M, Takahama Y, Yewdell JW, Cam M, and Bhandoola A (2019). Myc controls a distinct transcriptional program in fetal thymic epithelial cells that determines thymus growth. Nat. Commun 10, 5498. [PubMed: 31792212]

Dong M, Yan BP, Liao JK, Lam YY, Yip GW, and Yu CM (2010). Rhokinase inhibition: a novel therapeutic target for the treatment of cardiovascular diseases. Drug Discov. Today 15, 622–629. [PubMed: 20601092]

Dudakov JA, Khong DMP, Boyd RL, and Chidgey AP (2010). Feeding the fire: the role of defective bone marrow function in exacerbating thymic involution. Trends Immunol. 31, 191–198. [PubMed: 20356793]

Dudakov JA, Hanash AM, Jenq RR, Young LF, Ghosh A, Singer NV, West ML, Smith OM, Holland AM, Tsai JJ, et al. (2012). Interleukin-22 drives endogenous thymic regeneration in mice. Science 336, 91–95. [PubMed: 22383805]

Dudakov JA, Hanash AM, and van den Brink MR (2015). Interleukin-22: immunobiology and pathology. Annu. Rev. Immunol 33, 747–785. [PubMed: 25706098]

Dudakov JA, Perales MA, and van den Brink MRM (2016). Immune reconstitution following hematopoietic cell transplantation. In Thomas' Hematopoietic Cell Transplantation, Forman S, Negrin RS, Antin JH, and Appelbaum FA, eds. (Wiley), pp. 160–165.

Dudakov JA, Mertelsmann AM, O'Connor MH, Jenq RR, Velardi E, Young LF, Smith OM, Boyd RL, van den Brink MRM, and Hanash AM (2017). Loss of thymic innate lymphoid cells leads to impaired thymopoiesis in experimental graft-versus-host disease. Blood 130, 933–942. [PubMed: 28607133]

Dumont C, Corsoni-Tadrzak A, Ruf S, de Boer J, Williams A, Turner M, Kioussis D, and Tybulewicz VLJ (2009). Rac GTPases play critical roles in early T-cell development. Blood 113, 3990–3998. [PubMed: 19088377]

Flynn R, Paz K, Du J, Reichenbach DK, Taylor PA, Panoskaltsis-Mortari A, Vulic A, Luznik L, MacDonald KKP, Hill GR, et al. (2016). Targeted Rho-associated kinase 2 inhibition suppresses murine and human chronic GVHD through a Stat3-dependent mechanism. Blood 127, 2144–2154. [PubMed: 26983850]

Gomez M, Tybulewicz V, and Cantrell DA (2000). Control of pre-T cell proliferation and differentiation by the GTPase Rac-I. Nat. Immunol 1, 348–352. [PubMed: 11017108]

Gomez M, Kioussis D, and Cantrell DA (2001). The GTPase Rac-1 controls cell fate in the thymus by diverting thymocytes from positive to negative selection. Immunity 15, 703–713. [PubMed: 11728333]

Granadier D, Iovino L, Kinsella S, and Dudakov JA (2021). Dynamics of thymus function and T cell receptor repertoire breadth in health and disease. Semin. Immunopathol 43, 119–134. [PubMed: 33608819]

Gruver AL, and Sempowski GD (2008). Cytokines, leptin, and stress-induced thymic atrophy. J. Leukoc. Biol 84, 915–923. [PubMed: 18495786]

Guo F, Cancelas JA, Hildeman D, Williams DA, and Zheng Y (2008). Rac GTPase isoforms Rac1 and Rac2 play a redundant and crucial role in T-cell development. Blood 112, 1767–1775. [PubMed: 18579797]

Hernandez JB, Newton RH, and Walsh CM (2010). Life and death in the thymus–cell death signaling during T cell development. Curr. Opin. Cell Biol 22, 865–871. [PubMed: 20810263]

Hervé JC, and Bourmeyster N (2015). Rho GTPases at the crossroad of signaling networks in mammals. Small GTPases 6, 43–48. [PubMed: 26110743]

Hodge RG, and Ridley AJ (2016). Regulating Rho GTPases and their regulators. Nat. Rev. Mol. Cell Biol 17, 496–510. [PubMed: 27301673]

Huntzinger E, and Izaurralde E (2011). Gene silencing by microRNAs: contributions of translational repression and mRNA decay. Nat. Rev. Genet 12, 99–110. [PubMed: 21245828]

Hunziker L, Benitah SA, Braun KM, Jensen K, McNulty K, Butler C, Potton E, Nye E, Boyd R, Laurent G, et al. (2011). Rac1 deletion causes thymic atrophy. PLoS ONE 6, e19292. [PubMed: 21559396]

Iwanaga Y, Davey MP, Martin TM, Planck SR, DePriest ML, Baugh MM, Suing CM, and Rosenbaum JT (2003). Cloning, sequencing and expression analysis of the mouse NOD2/CARD15 gene. Inflamm. Res 52, 272–276. [PubMed: 12835899]

Jaffe HL (1924). The Influence of the Suprarenal Gland on the Thymus: I. Regeneration of the Thymus Following Double Suprarenalectomy in the Rat. J. Exp. Med 40, 325–342. [PubMed: 19868921]

Jagasia M, Lazaryan A, Bachier CR, Salhotra A, Weisdorf DJ, Zoghi B, Essell J, Green L, Schueller O, Patel J, et al. (2021). ROCK2 Inhibition With Belumosudil (KD025) for the Treatment of Chronic Graft-Versus-Host Disease. J. Clin. Oncol 39, 1888–1898. [PubMed: 33877856]

Jameson SC, Hogquist KA, and Bevan MJ (1995). Positive selection of thymocytes. Annu. Rev. Immunol 13, 93–126. [PubMed: 7612239]

Keestra AM, Winter MG, Auburger JJ, Frässle SP, Xavier MN, Winter SE, Kim A, Poon V, Ravesloot MM, Waldenmaier JFT, et al. (2013). Manipulation of small Rho GTPases is a pathogen-induced process detected by NOD1. Nature 496, 233–237. [PubMed: 23542589]

Keestra-Gounder AM, and Tsolis RM (2017). NOD1 and NOD2: Beyond Peptidoglycan Sensing. Trends Immunol. 38, 758–767. [PubMed: 28823510]

Kinnebrew MA, Buffie CG, Diehl GE, Zenewicz LA, Leiner I, Hohl TM, Flavell RA, Littman DR, and Pamer EG (2012). Interleukin 23 production by intestinal CD103(+)CD11b(+) dendritic cells in response to bacterial flagellin enhances mucosal innate immune defense. Immunity 36, 276–287. [PubMed: 22306017]

Kinsella S, and Dudakov JA (2020). When the Damage Is Done: Injury and Repair in Thymus Function. Front. Immunol 11, 1745. [PubMed: 32903477]

Komanduri KV, St John LS, de Lima M, McMannis J, Rosinski S, McNiece I, Bryan SG, Kaur I, Martin S, Wieder ED, et al. (2007). Delayed immune reconstitution after cord blood transplantation is characterized by impaired thymopoiesis and late memory T-cell skewing. Blood 110, 4543–4551. [PubMed: 17671230]

Koyanagi M, Takahashi J, Arakawa Y, Doi D, Fukuda H, Hayashi H, Narumiya S, and Hashimoto N (2008). Inhibition of the Rho/ROCK pathway reduces apoptosis during transplantation of embryonic stem cell-derived neural precursors. J. Neurosci. Res 86, 270–280. [PubMed: 17828770]

Krieser RJ, and Eastman A (1999). Cleavage and nuclear translocation of the caspase 3 substrate Rho GDP-dissociation inhibitor, D4-GDI, during apoptosis. Cell Death Differ. 6, 412–419. [PubMed: 10381642]

Krol J, Loedige I, and Filipowicz W (2010). The widespread regulation of microRNA biogenesis, function and decay. Nat. Rev. Genet 11, 597–610. [PubMed: 20661255]

Lacal JC (1997). Regulation of proliferation and apoptosis by Ras and Rho GTPases through specific phospholipid-dependent signaling. FEBS Lett. 410, 73–77. [PubMed: 9247126]

Legrand N, Dontje W, van Lent AU, Spits H, and Blom B (2007). Human thymus regeneration and T cell reconstitution. Semin. Immunol 19, 280–288. [PubMed: 17997107]

Legrand-Poels S, Kustermans G, Bex F, Kremmer E, Kufer TA, and Piette J (2007). Modulation of Nod2-dependent NF-kappaB signaling by the actin cytoskeleton. J. Cell Sci 120, 1299–1310. [PubMed: 17356065]

Lemke G, and Rothlin CV (2008). Immunobiology of the TAM receptors. Nat. Rev. Immunol 8, 327–336. [PubMed: 18421305]

Lin Y, and Zheng Y (2015). Approaches of targeting Rho GTPases in cancer drug discovery. Expert Opin. Drug Discov 10, 991–1010. [PubMed: 26087073]

Mackall CL (2000). T-cell immunodeficiency following cytotoxic antineoplastic therapy: a review. Stem Cells 18, 10–18. [PubMed: 10661568]

Mackall CL, Fleisher TA, Brown MR, Andrich MP, Chen CC, Feuerstein IM, Horowitz ME, Magrath IT, Shad AT, Steinberg SM, et al. (1995). Age, thymopoiesis, and CD4+ T-lymphocyte regeneration after intensive chemotherapy. N. Engl. J. Med 332, 143–149. [PubMed: 7800006]

Mak TW, Penninger JM, and Ohashi PS (2001). Knockout mice: a paradigm shift in modern immunology. Nat. Rev. Immunol 1, 11–19. [PubMed: 11905810]

Makeyev EV, and Maniatis T (2008). Multilevel regulation of gene expression by microRNAs. Science 319, 1789–1790. [PubMed: 18369137]

Mao Y, and Finnemann SC (2015). Regulation of phagocytosis by Rho GTPases. Small GTPases 6, 89–99. [PubMed: 25941749]

Martinic MM, Caminschi I, O'Keeffe M, Thinnes TC, Grumont R, Gerondakis S, McKay DB, Nemazee D, and Gavin AL (2017). The Bacterial Peptidoglycan-Sensing Molecules NOD1 and NOD2 Promote CD8+ Thymocyte Selection. J. Immunol 198, 2649–2660. [PubMed: 28202617]

Mazieres J, Pradines A, and Favre G (2004). Perspectives on farnesyl transferase inhibitors in cancer therapy. Cancer Lett. 206, 159–167. [PubMed: 15013521]

Miller JF (1961). Immunological function of the thymus. Lancet 2, 748–749. [PubMed: 14474038]

Miller JFAP (2020). The function of the thymus and its impact on modern medicine. Science 369, eaba2429. [PubMed: 32732394]

Mower DA Jr., Peckham DW, Illera VA, Fishbaugh JK, Stunz LL, and Ashman RF (1994). Decreased membrane phospholipid packing and decreased cell size precede DNA cleavage in mature mouse B cell apoptosis. J. Immunol 152, 4832–4842. [PubMed: 8176206]

Municio C, Hugo E, Alvarez Y, Alonso S, Blanco L, Fernández N, and Sánchez Crespo M (2011). Apoptotic cells enhance IL-10 and reduce IL-23 production in human dendritic cells treated with zymosan. Mol. Immunol 49, 97–106. [PubMed: 21872333]

Na S, Chuang TH, Cunningham A, Turi TG, Hanke JH, Bokoch GM, and Danley DE (1996). D4-GDI, a substrate of CPP32, is proteolyzed during Fas-induced apoptosis. J. Biol. Chem 271, 11209–11213. [PubMed: 8626669]

Nunes-Alves C, Nobrega C, Behar SM, and Correia-Neves M (2013). Tolerance has its limits: how the thymus copes with infection. Trends Immunol. 34, 502–510. [PubMed: 23871487]

Papadopoulou AS, Dooley J, Linterman MA, Pierson W, Ucar O, Kyewski B, Zuklys S, Hollander GA, Matthys P, Gray DHD, et al. (2011). The thymic epithelial microRNA network elevates the threshold for infection-associated thymic involution via miR-29a mediated suppression of the IFN-α receptor. Nat. Immunol 13, 181–187. [PubMed: 22179202]

Parikh P, Hao Y, Hosseinkhani M, Patil SB, Huntley GW, Tessier-Lavigne M, and Zou H (2011). Regeneration of axons in injured spinal cord by activation of bone morphogenetic protein/Smad1 signaling pathway in adult neurons. Proc. Natl. Acad. Sci. USA 108, E99–E107. [PubMed: 21518886]

Parkman R, and Weinberg KI (1997). Immunological reconstitution following bone marrow transplantation. Immunol. Rev 157, 73–78. [PubMed: 9255623]

Pizzo PA, Rubin M, Freifeld A, and Walsh TJ (1991). The child with cancer and infection. II. Nonbacterial infections. J. Pediatr 119, 845–857. [PubMed: 1660069]

Purton JF, Monk JA, Liddicoat DR, Kyparissoudis K, Sakkal S, Richardson SJ, Godfrey DI, and Cole TJ (2004). Expression of the glucocorticoid receptor from the 1A promoter correlates with T lymphocyte sensitivity to glucocorticoid-induced cell death. J. Immunol 173, 3816–3824. [PubMed: 15356129]

Ricker E, Chowdhury L, Yi W, and Pernis AB (2016). The RhoA-ROCK pathway in the regulation of T and B cell responses. F1000Res. 2016, 5.

Rothlin CV, Ghosh S, Zuniga EI, Oldstone MB, and Lemke G (2007). TAM receptors are pleiotropic inhibitors of the innate immune response. Cell 131, 1124–1136. [PubMed: 18083102]

Rothlin CV, Carrera-Silva EA, Bosurgi L, and Ghosh S (2015). TAM receptor signaling in immune homeostasis. Annu. Rev. Immunol 33, 355–391. [PubMed: 25594431]

Sadok A, McCarthy A, Caldwell J, Collins I, Garrett MD, Yeo M, Hooper S, Sahai E, Kuemper S, Mardakheh FK, and Marshall CJ (2015). Rho kinase inhibitors block melanoma cell migration and inhibit metastasis. Cancer Res. 75, 2272–2284. [PubMed: 25840982]

Sanno H, Shen X, Kuru N, Bormuth I, Bobsin K, Gardner HA, Komljenovic D, Tarabykin V, Erzurumlu RS, and Tucker KL (2010). Control of postnatal apoptosis in the neocortex by RhoA-subfamily GTPases determines neuronal density. J. Neurosci 30, 4221–4231. [PubMed: 20335457]

Schlegel RA, Stevens M, Lumley-Sapanski K, and Williamson P (1993). Altered lipid packing identifies apoptotic thymocytes. Immunol. Lett 36, 283–288. [PubMed: 8370600]

Schmidt-Bleek K, Willie BM, Schwabe P, Seemann P, and Duda GN (2016). BMPs in bone regeneration: Less is more effective, a paradigm-shift. Cytokine Growth Factor Rev 27, 141–148. [PubMed: 26678813]

Seandel M, Butler JM, Kobayashi H, Hooper AT, White IA, Zhang F, Vertes EL, Kobayashi M, Zhang Y, Shmelkov SV, et al. (2008). Generation of a functional and durable vascular niche by the adenoviral E4ORF1 gene. Proc. Natl. Acad. Sci. USA 105, 19288–19293. [PubMed: 19036927]

Shang X, Marchioni F, Sipes N, Evelyn CR, Jerabek-Willemsen M, Duhr S, Seibel W, Wortman M, and Zheng Y (2012). Rational design of small molecule inhibitors targeting RhoA subfamily Rho GTPases. Chem. Biol 19, 699–710. [PubMed: 22726684]

Shutes A, Onesto C, Picard V, Leblond B, Schweighoffer F, and Der CJ (2007). Specificity and mechanism of action of EHT 1864, a novel small molecule inhibitor of Rac family small GTPases. J. Biol. Chem 282, 35666–35678. [PubMed: 17932039]

Todt JC, Hu B, and Curtis JL (2004). The receptor tyrosine kinase MerTK activates phospholipase C gamma2 during recognition of apoptotic thymocytes by murine macrophages. J. Leukoc. Biol 75, 705–713. [PubMed: 14704368]

Ucar O, Tykocinski LO, Dooley J, Liston A, and Kyewski B (2013). An evolutionarily conserved mutual interdependence between Aire and microRNAs in promiscuous gene expression. Eur. J. Immunol 43, 1769–1778. [PubMed: 23589212]

Van Aelst L, and D'Souza-Schorey C (1997). Rho GTPases and signaling networks. Genes Dev. 11, 2295–2322. [PubMed: 9308960]

van den Brink M, Uhrberg M, Jahn L, DiPersio JF, and Pulsipher MA (2018). Selected biological issues affecting relapse after stem cell transplantation: role of T-cell impairment, NK cells and intrinsic tumor resistance. Bone Marrow Transplant. 53, 949–959. [PubMed: 29367714]

van den Broek T, Delemarre EM, Janssen WJM, Nievelstein RAJ, Broen JC, Tesselaar K, Borghans JAM, Nieuwenhuis EES, Prakken BJ, Mokry M, et al. (2016). Neonatal thymectomy reveals differentiation and plasticity within human naive T cells. J. Clin. Invest 126, 1126–1136. [PubMed: 26901814]

Velardi E, Tsai JJ, Holland AM, Wertheimer T, Yu VWC, Zakrzewski JL, Tuckett AZ, Singer NV, West ML, Smith OM, et al. (2014). Sex steroid blockade enhances thymopoiesis by modulating Notch signaling. J Exp Med 211, 2341–2349. [PubMed: 25332287]

Velardi E, Tsai JJ, and van den Brink MRM (2020). T cell regeneration after immunological injury. Nat. Rev. Immunol.

Wallet MA, Flores RR, Wang Y, Yi Z, Kroger CJ, Mathews CE, Earp HS, Matsushima G, Wang B, and Tisch R (2009). MerTK regulates thymic selection of autoreactive T cells. Proc. Natl. Acad. Sci. USA 106, 4810–4815. [PubMed: 19251650]

Weinberg K, Annett G, Kashyap A, Lenarsky C, Forman SJ, and Parkman R (1995). The effect of thymic function on immunocompetence following bone marrow transplantation. Biol. Blood Marrow Transplant. 1, 18–23. [PubMed: 9118285]

Wennerberg K, and Der CJ (2004). Rho-family GTPases: it's not only Rac and Rho (and I like it). J. Cell Sci. 117, 1301–1312. [PubMed: 15020670]

Wertheimer T, Velardi E, Tsai J, Cooper K, Xiao S, Kloss CC, Ottmüller KJ, Mokhtari Z, Brede C, deRoos P, et al. (2018). Production of BMP4 by endothelial cells is crucial for endogenous thymic regeneration. Sci. Immunol 3, eaal2736. [PubMed: 29330161]

Williams KM, Hakim FT, and Gress RE (2007). T cell immune reconstitution following lymphodepletion. Semin. Immunol 19, 318–330. [PubMed: 18023361]

Wu Y, Singh S, Georgescu MM, and Birge RB (2005). A role for Mer tyrosine kinase in alphavbeta5 integrin-mediated phagocytosis of apoptotic cells. J. Cell Sci 118, 539–553. [PubMed: 15673687]

Ye Y, Li D, Ouyang D, Deng L, Zhang Y, Ma Y, and Li Y (2014). MicroRNA expression in the aging mouse thymus. Gene 547, 218–225. [PubMed: 24956559]

Yokoyama Y, Lew ED, Seelige R, Tindall EA, Walsh C, Fagan PC, Lee JY, Nevarez R, Oh J, Tucker KD, et al. (2019). Immuno-Oncological Efficacy of RXDX-106, a Novel Small Molecule Inhibitor of the TAM (TYRO3, AXL, MER) Family of Kinases. Cancer Res. 79, 1996–2008. [PubMed: 30723115]

Zanin-Zhorov A, Weiss JM, Nyuydzefe MS, Chen W, Scher JU, Mo R, Depoil D, Rao N, Liu B, Wei J, et al. (2014). Selective oral ROCK2 inhibitor down-regulates IL-21 and IL-17 secretion in human T cells via STAT3-dependent mechanism. Proc. Natl. Acad. Sci. USA 111, 16814–16819. [PubMed: 25385601]

Zheng Y, Danilenko DM, Valdez P, Kasman I, Eastham-Anderson J, Wu J, and Ouyang W (2007). Interleukin-22, a T(H)17 cytokine, mediates IL-23-induced dermal inflammation and acanthosis. Nature 445, 648–651. [PubMed: 17187052]

Highlights

- NOD2 suppresses the production of the key thymic regenerative factors BMP4 and IL-23
- Detection of apoptotic thymocytes by TAM receptors mediates NOD2-dependent suppression
- Depletion of thymocytes after acute damage attenuates detection of apoptotic cells
- Inhibition of Rac1 promotes thymus repair and T cell reconstitution after damage

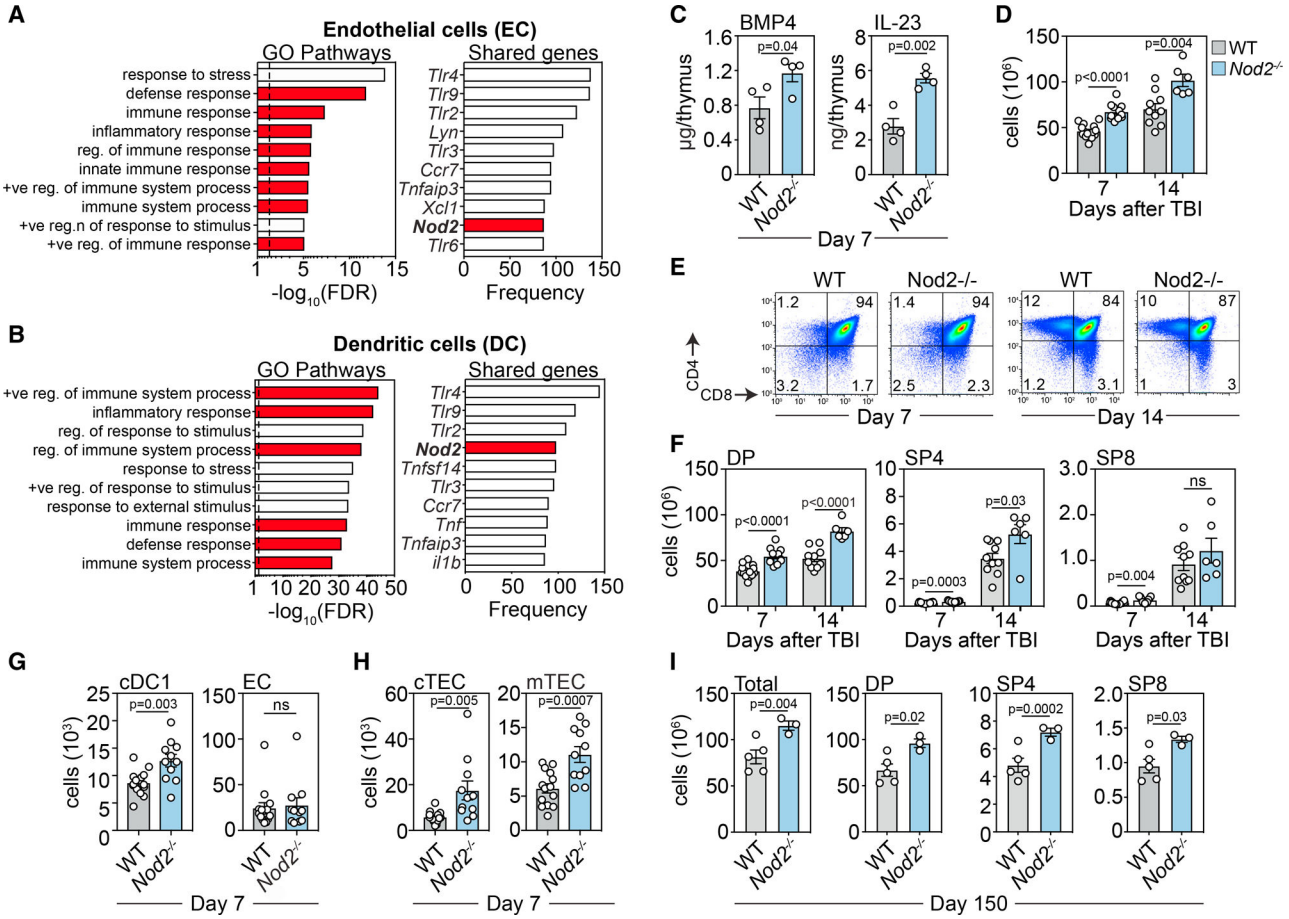

Figure 1. NOD2 limits thymus regeneration by inhibiting the production of regenerative factors

(A and B) Thymuses were pooled from 6-week-old C57BL/6 mice, and transcriptome analysis was performed on fluorescence-activated cell sorting (FACS)-purified ECs (A) or DCs (B) isolated from either untreated mice (d0) or 4 days after TBI (550 cGy, d0, n = 3; d4, n = 2; each n pooled from 5 mice). (A) Gene ontology (GO) pathway analysis was performed on upregulated genes in ECs at day 4 after SL-TBI using DAVID, and the top-ten pathways by FDR are displayed. Red bars represent pathways involved with immune function; dashed line at p = 0.05. Top-ten genes in ECs are shown by frequency of representation among all GO pathways with an FDR <0.05. (B) Gene ontology (GO) pathway analysis was performed on upregulated genes in DCs at day 4 after SL-TBI using DAVID, and the top-ten pathways by FDR are displayed. Red bars represent pathways involved with immune function; dashed line at p = 0.05. Top-ten genes in DCs are shown by frequency of representation among all GO pathways with an FDR <0.05.

(C–I) 6- to 8-week C57BL/6 WT or *Nod2*$^{-/-}$ mice were given a sublethal dose of TBI (550 cGy), and the thymus was harvested and analyzed at the indicated time points. (C) Total thymic amounts of BMP4, IL-23, and IL-22 were assessed by ELISA at day 7 after SL-TBI (n = 4/group from a representative experiment of at least two independent experiments). (D) Total thymic cellularity at days 7 and 14 after SL-TBI (d7, n = 11–15; d14, n = 6–10; combined from two independent experiments). (E) Concatenated flow plots showing CD4 and CD8 expression at days 7 and 14 after SL-TBI. (F) Total

number of $CD4^+CD8^+$ DP, $CD4^+CD3^+$ SP4, or $CD3^+CD8^+$ SP8 thymocytes (d7, n = 11–15; d14, n = 6–10; combined from two independent experiments). (G) Number of $CD45^+MHCII^+CD11c^+CD103^+$ cDC1 and $CD45^-EpCAM^-CD31^+PDGFRa^-$ ECs at day 7 after SL-TBI (n = 11–15/group across two independent experiments). (H) Number of $CD45^-EpCAM^+MHCII^+UEA1^{lo}Ly51^{hi}$ cTECs and $CD45^-EpCAM^+MH\text{-}CII^+UEA1^{hi}Ly51^{lo}$ mTECs at day 7 after SL-TBI (n = 11–15/group across two independent experiments). (I) Total thymic cellularity and absolute number of thymocyte subsets at day 150 after SL-TBI (n = 3–5). Graphs represent mean ± SEM; each dot represents a biologically independent observation. See also Figures S1 and S2.

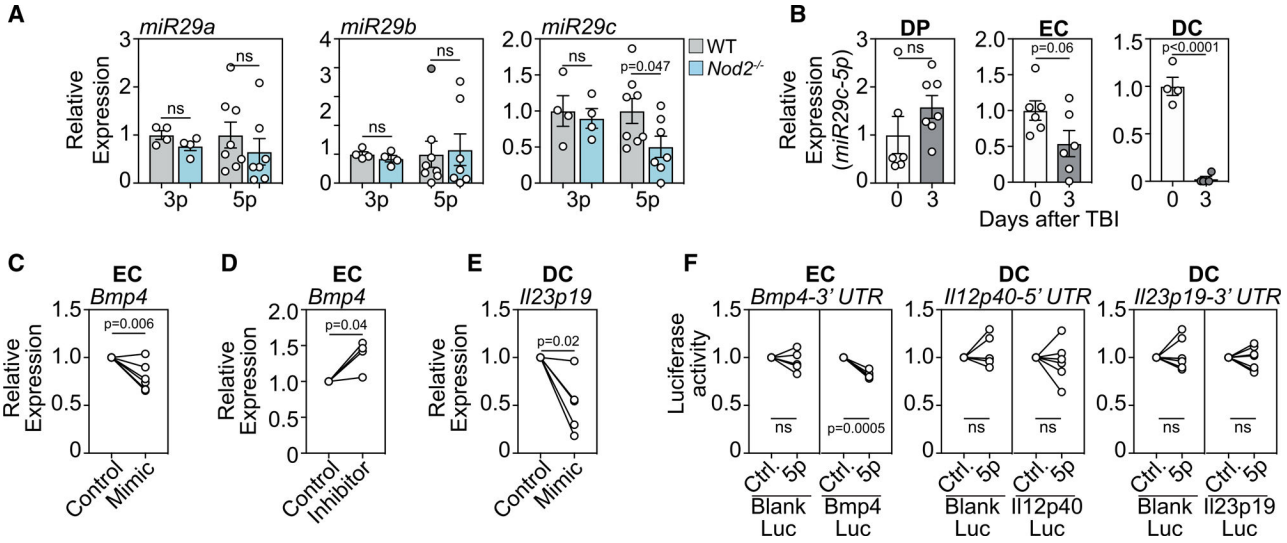

Figure 2. miR29c mediates the effects of NOD2 in limiting production of regenerative factors in ECs and DCs

(A) Thymuses were isolated from 6- to 8-week C57BL/6 WT or *Nod2*$^{-/-}$ mice at day 3 following SL-TBI, and the expression of 3p and 5p arms of *miR29a*, *miR29b*, or *miR29c* was analyzed by qPCR (3p, n = 4/group; 5p, n = 7/group across two independent experiments).

(B) DPs, ECs, and DCs were FACS purified from WT thymuses at day 0 or 3 after SL-TBI and expression of *miR29c-5p* was analyzed by qPCR (DCs, n = 4; ECs/DPs, n = 6–7/population/time point across two independent experiments).

(C) Thymic exECs were generated as previously described (Seandel et al., 2008; Wertheimer et al., 2018) and transfected with a miR29c mimic. 20 h after transfection, the expression of *Bmp4* was analyzed by qPCR (n = 7 independent experiments).

(D) exECs were transfected with a *miR29c* inhibitor, and the expression of *Bmp4* was analyzed by qPCR 20 h after transfection (n = 4 independent experiments).

(E) CD11c^{+} DCs were isolated from untreated C57BL/6 thymuses and transfected with a miR29c mimic. 20 h after transfection, *Il23p19* was analyzed by qPCR (n = 5 across three independent experiments).

(F) HEK293 cells were co-transfected with either *Bmp4*-3′ UTR, *Il12p40*-5′ UTR, or *Il23p19*-3′ UTR luciferase constructs and a *miR29c-5p* mimic. Binding activity was quantified by measuring luciferase activity after 20 h (n = 5–7 independent experiments).

Graphs represent mean ± SEM; each dot represents a biologically independent observation. See also Figure S3.

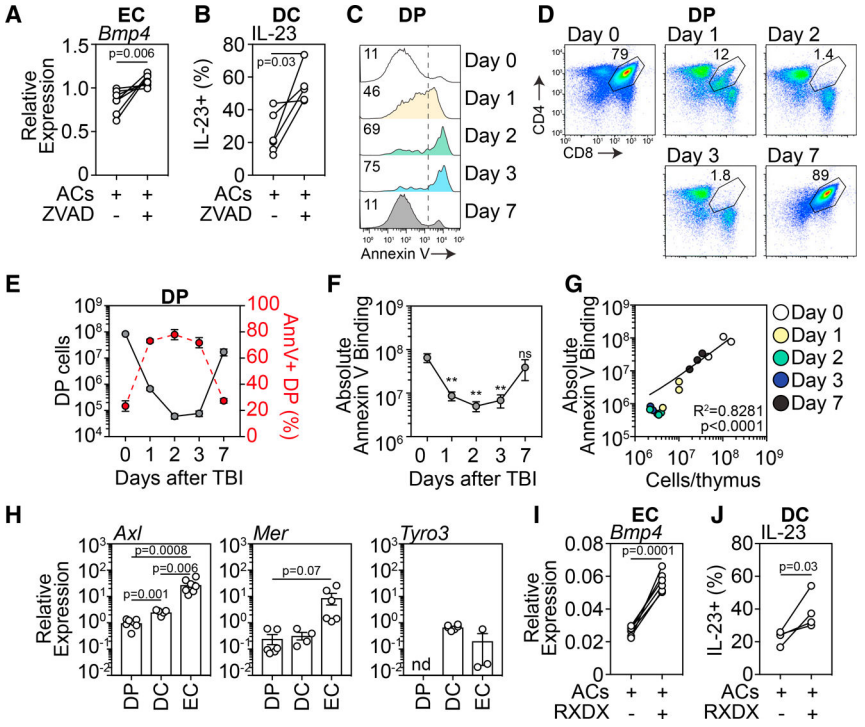

Figure 3. TAM receptor detection of phosphatidylserine mediates thymocyte suppression of regenerative factors

(A and B) Thymocytes were isolated from untreated C57BL/6 mice and incubated for 4 h with Dexamethasone (100 nM) or zVAD-FMK (20 μM). After 4 h, apoptotic thymocytes (ACs) were washed and co-cultured with exECs (A) or freshly isolated CD11c^{+} DCs (B) for 24 h after which *Bmp4* expression was analyzed by qPCR (n = 7 across 5 independent experiments) or IL-23 was analyzed by intracellular cytokine staining (n = 5 across two independent experiments).

(C–G) 6- to 8-week-old C57BL/6 mice were given sublethal TBI (550 cGy), and the thymus was harvested at days 0, 1, 2, 3, and 7. (C) Annexin V staining on DP thymocytes (displayed are concatenated plots from 3 individual mice, representative of three independent experiments). (D) Staining for CD4 and CD8 on thymus cells (displayed are concatenated plots from 3 individual mice, representative of three independent experiments). (E) Total number of DP thymocytes (solid line; left axis) compared with proportion of Annexin V^{+} DP thymocytes (red broken line; right axis) (n = 8 across 3 independent experiments). (F) Absolute binding of Annexin V in the thymus (n = 8 across 3 independent experiments). (G) Correlation of absolute thymic binding of Annexin V with total number of cells in the thymus (n = 3/time point comprising one of three independent experiments).

(H) DP thymocytes, DCs, or ECs were FACS purified from untreated C57BL/6 mice, and expression of *Axl, Mer*, and *Tyro3* was analyzed by qPCR (DP, n = 7; DC, n = 5; EC, n = 7 across two independent experiments).

(I and J) Thymocytes were isolated from untreated C57BL/6 mice and incubated for 4 h with dexamethasone (100 nM). After 4 h, apoptotic thymocytes (ACs) were washed and co-cultured with exECs (I) or freshly isolated CD11c^{+} DCs. (J) in the presence or absence of the TAM receptor inhibitor RXDX-106 (25 μM) for 20 h after which *Bmp4* expression

was analyzed by qPCR (n = 6/treatment across 2 independent experiments) or IL-23 was analyzed by intracellular cytokine staining (n = 4). Graphs represent mean ± SEM; each dot represents a biologically independent observation. See also Figure S4.

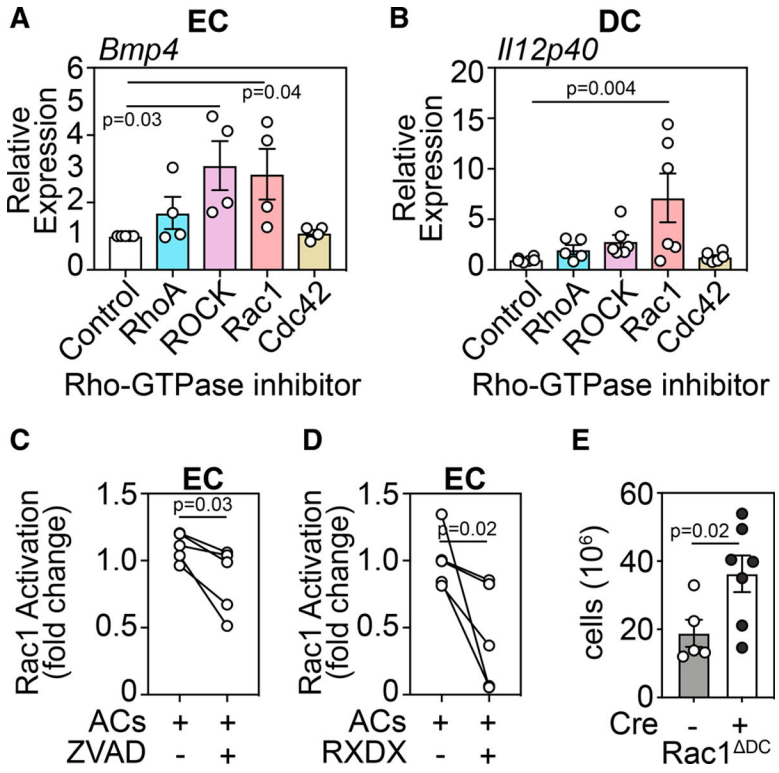

Figure 4. Rac1-GTPase is activated by apoptotic thymocytes and suppresses production of IL-23 and BMP4

(A and B) exECs (A) or freshly isolated CD11c^{+} DCs (B) were incubated for 20 h in the presence of inhibitors (all at 50 μM) for RhoA (Rhosin), ROCK (TC-S 7001), Rac1 (EHT-1864), or Cdc42 (ZCL272) after which *Bmp4* (ECs) or *Il12p40* was analyzed by qPCR (exECs, n = 5 independent experiments; DCs, n = 6 across two independent experiments).

(C) Thymocytes were isolated from untreated C57BL/6 mice and incubated for4 h with Dexamethasone (100 nM) or zVAD-FMK (20 μM). After 4 h, apoptotic thymocytes (ACs) were washed and co-cultured with exECs for 24 h after which Rac1-GTPase activation was measured using a GTPase ELISA specific for Rac1 (n = 5 across two independent experiments).

(D) Thymocytes were isolated from untreated C57BL/6 mice and incubated for 4 h with dexamethasone (100 nM). After 4 h, apoptotic thymocytes (ACs) were washed and co-cultured with exECs in the presence or absence of the TAM receptor inhibitor RXDX-106 (25 μM) for 20 h after which Rac1-GTPase activation was measured using a GTPase ELISA specific for Rac1 (n = 5 across two independent experiments).

(E) Mice deficient for Rac1 specifically in DCs were generated by crossing Rac1$^{fl/fl}$ mice with CD11c-Cre. WT or Rac1$^{\Delta DC}$ mice were given SL-TBI and thymus cellularity was assessed at day 7 (n = 5–7/group combined from two independent experiments). Graphs represent mean ± SEM; each dot represents a biologically independent observation.

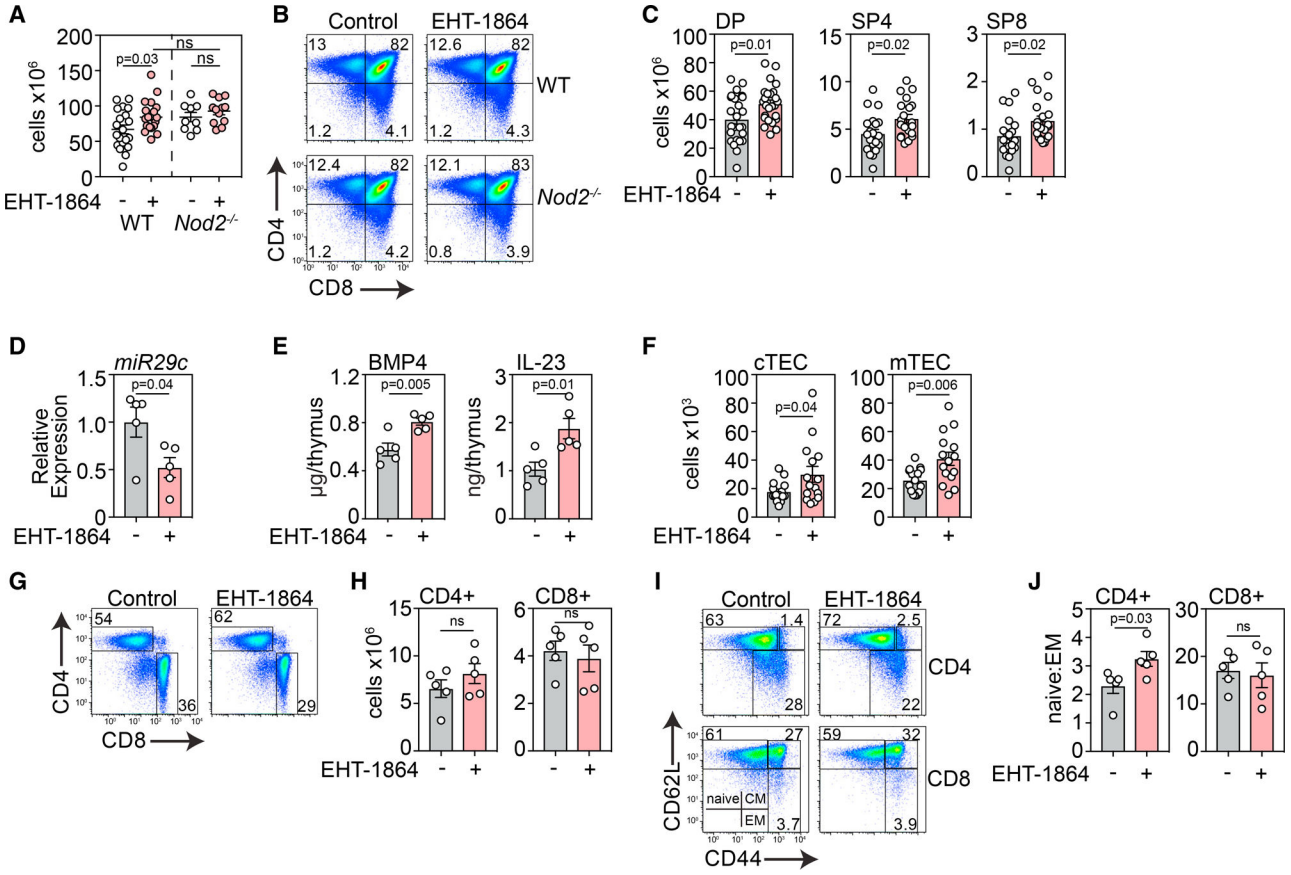

Figure 5. Rac1 inhibition enhances thymus regeneration and peripheral CD4$^+$ naive T cell recovery after acute damage

6- to 8-week C57BL/6 WT or *Nod2*$^{-/-}$ mice were treated with the Rac1 inhibitor EHT1864 (40 mg/kg i.p. injection) at days 3, 5, and 7 following a sublethal dose of TBI (550 cGy), and the thymus was analyzed on day 14.

(A) Total thymic cellularity at day 14 after SL-TBI (WT, n = 20/treatment across 4 independent experiments; KO, n = 9–12 across three independent experiments).

(B) Flow plots showing CD4 and CD8 expression at day 14 after SL-TBI (gated on CD45$^+$ cells; plots were concatenated of all samples in each treatment group from one experiment).

(C) Total number of DP, SP4, or SP8 thymocytes (n = 20/treatment across 4 independent experiments).

(D) Expression of *miR29c* analyzed by qPCR on whole thymic tissue (n = 5/group).

(E) Total thymic amounts of BMP4 and IL-23 assessed by ELISA at day 7 (n = 4–5/group, representative of two independent experiments).

(F) Total number of cTECs and mTECs (n = 15/group across three independent experiments).

(G) Flow plots showing CD4 and CD8 expression in the spleen at day 56 after SL-TBI (gated on CD45$^+$CD3$^+$ cells).

(H) Total number of CD4$^+$ and CD8$^+$ T cells in the spleen at d56 (n = 5/group).

(I) Plots of CD62L and CD44 on $CD4^+$ and $CD8^+$ T cells (gated on either $CD45^+CD3^+CD4^+CD8^-$ or $CD45^+CD3^+CD4^-CD8^+$) cells; plots concatenated of all samples in a given experiment).
(J) Ratio of number of naive ($CD62L^{hi}$ $CD44^{lo}$) $CD4^+$ or $CD8^+$ to $CD4^+$ or $CD8^+$ EM ($CD62L^{hi}$ $CD44^{hi}$) T cells (n = 5/group).
Experiments in (C)–(J) were performed only in WT mice. Graphs represent mean ± SEM; each dot represents a biologically independent observation. See also Figure S5.

KEY RESOURCES TABLE

Reagent or resource	Source	Identifier
Antibodies		
CD3-FITC	Tonbo Biosciences	35-0031; RRID:AB_2621659
CD8-BV711	BioLegend	100748; RRID:AB_2562100
CD4-BV650	BioLegend	100546; RRID:AB_2562098
CD45-BUV395	BD Biosciences	565967; RRID:AB_2739420
CD90-BV785	BioLegend	105331; RRID:AB_2562900
CD11c-APC	Tonbo Biosciences	20-0114; RRID:AB_2621557
MHC-II-Pac Blue	BioLegend	107620; RRID:AB_493527
CD103-PercPCy5.5	BioLegend	121416; RRID:AB_2128621
CD11b-A700	BD PharMingen	557960; RRID:AB_396960
EpCAM-PercPe710	eBioscience	46-5791-82; RRID:AB_10598205
Ly51-PE	eBioscience	12-5891-83; RRID:AB_466016
CD31-PECy7	eBioscience	25-0311-82; RRID:AB_2716949
CD140a-APC	BioLegend	135907; RRID:AB_2043969
UEA1-FITC	Vector Laboratories	FL-1061; RRID:AB_2336767
TCRbetaPECy7	BioLegend	109222; RRID:AB_893625
CD62L-APC-Cy7	BioLegend	104427; RRID:AB_830798
CD44-Alexa Fluor RTM700	eBioscience	56-0441-82; RRID:AB_494011
CD25-PercP-Cy5.5	BioLegend	102030; RRID:AB_893288
Annexin V	BioLegend	640906
Bacterial and virus strains		
DH5alpha competent cells	Sigma	18265017
Biological samples		
Mouse: thymus & spleen harvested from C57BL/6J & B6.129S1-Nod2tm1Flv/J mice	This paper	N/A
Chemicals, peptides, and recombinant proteins		
EHT1864	Tocris, UK	3872

Reagent or resource	Source	Identifier
RXDX-106 (CEP-40783)	Selleck Chemicals	s8570
z-VAD-FMK	Tocris, UK	2163
Dexamethasone	Sigma Aldrich, Germany	D2915
Lipofectamine 2000	Thermo fisher	11668019
RNAifectin	Abm, Btitish Columbia, Canada	G073
OptiMEM reduced serum media	GIBCO	31985070
Critical commercial assays		
BMP4 ELISA	R&D systems	DY485-05
IL-23 ELISA	BioLegend	433704
G-LISA Rac1 Activation Assay Biochem Kit	Cytoskeleton, USA	BK128
Pierce BCA protein assay kit	Thermo Fisher	23227
RNeasy Mini kit	QIAGEN	74104
Rneasy Plus Micro Kit	QIAGEN	74034
miRNeasy Mini kit	QIAGEN	217004
miRNeasy Micro kit	QIAGEN	1071023
iScript gDNA Clear cDNA synthesis kit	Bio-Rad	1725035
Dual-Glo® Luciferase Assay System	Promega	E2920
iTaq Universal SYBR Green Supermix	Bio-Rad	1725122
Taqman Advanced miRNA cDNA Synthesis kit	Thermo Fisher	A28007
Nucleofector endothelial electroporation kit	Lonza	VPI-1001
Deposited data		
EC microarray data (Day 0)	Wertheimer et al. (2018)	GEO: GSE106982
EC microarray data (Day 4)	This paper	GEO: GSE160989
DC RNA sequencing	This paper	GEO: GSE183056
Experimental models: Cell lines		
exEC: purified thymic endothelial cells transduced with pCCL-PGK-myrAkt vector	Brandon Hadland, Fred Hutchinson Cancer Research Center	N/A
exEC: purified thymic endothelial cells transduced with E4orf1 viral gene	Shahin Rafii, Weill Cornell Medical College	N/A

Reagent or resource	Source	Identifier
HEK293	ATCC	CRL-1573
Experimental models: Organisms/strains		
Mouse: C57BL/6J	Jackson Laboratories	0006644
Mouse: Nod2−/− (B6.129S1-Nod2tm1Flv/J)	Jackson Laboratories	005763
Mouse: Rac1fl/fl*CD11c Cre	Jackson Laboratories	Rac1fl/fl, 005550; CD11c-cre, 007567
Oligonucleotides		
B-Actin – F (CACTGTCGAGTCGCGTCC)	IDT	N/A
B-Actin – R (TCATCCATGGCGAACTGGTG)	IDT	N/A
Il12p40 – F (AAGGAACAGTGGGTGTCCAG)	IDT	N/A
Il12p40 – R (CATCTTCTTCAGGCGTGTCA)	IDT	N/A
Il23p19 – F (GACTCAGCCAACTCCTCCAG)	IDT	N/A
Il23p19 – R (GGCACTAAGGGCTCAGTCAG)	IDT	N/A
Bmp4	Bio-Rad	qMmuCED0046239
miR29a-3p	Thermo Fisher	mmu478587_mir
miR29b-3p	Thermo Fisher	mmu481300_mir
miR29c-3p	Thermo Fisher	mmu479229_mir
miR29a-5p	Thermo Fisher	mmu481032_mir
miR29b-5p	Thermo Fisher	mmu481675_mir
miR29c-5p	Thermo Fisher	mmu481034_mir
Recombinant DNA		
pLenti-Ubc-UTR-Dual-Luc-Blank	Abm custom vector	N/A
pLenti-Ubc-3′UTR-Dual-Luciferase (GAATTCACTAGTACCGGTAGGCCTGTCGACGATATCGGGCCCGCGGCCGCTGGATCCTCTAGACTCGAG)	Abm custom vector	N/A
pLenti-Ubc-IL12B-5′UTR-Dual-luciferase (GGCGCGCCACTAGTACCGGTAGGCCTGTCGACGATATCGGGCCCGCGGCCGCTGGATCC)	Abm custom vector	N/A
pLenti-Ubc-IL23A-3′UTR-Dual-Luciferase (GGATTCACTAGTACCGGTAGGCCTGTCGACGATATCGGGCCCGCGGCCGCTGGATCCTCTAGACTCGAG)	Abm custom vector	N/A
pCCL-PGK-myrAkt vector	Brandon Hadland, Fred Hutchinson Cancer Research Center	N/A
Software and algorithms		

Reagent or resource	Source	Identifier
GSEA tool v4.1	Broad Institute	https://www.gsea-msigdb.org/gsea
Prism v8.0	GraphPad Software	https://www.graphpad.com
FlowJo v9	BD	https://www.flowjo.com/
BioRender	BioRender	https://app.biorender.com
Other		
TECAN Spark 10M	Tecan, Switzerland	Spark 10M
Z2 Coulter Particle and Size Analyzer	Beckman Coulter, USA	N/A
Bio-Rad CFX96 Real Time System	Bio-Rad	N/A
Luminometer	Turner Biosystems, USA	Veritas microplate Luminometer
Amaxa Nucleofector (Program M-003)	Lonza	Nucleofecotr 2b
Irradiator	Fred Hutchinson Cancer Research Center	Mark I series 30JL Shepherd irradiator